Th C 02

Reflection FWI in MBTT Formulation: Macro Velocity Reconstruction

V. Tcheverda* (Institute of Petroleum Geology & Geophysics SB RAS), K. Gadylshin (Institute of Petroleum Geology and Geophysics), G. Chavent (INRIA), C. Shin (Seoul National University) & J. Shin (Seoul National University)

SUMMARY

Unfortunately we have to admit that after decades of development there are still no reliable techniques of full waveform inversion which guarantee reliable reconstruction of both macrovelocity model and reflectors reconstruction for reasonable acquisitions and frequency ranges. As reasonable we mean realistic offsets (about one-two depths of target objects) and temporal frequency above 5 – 7 Hz.

The paper is devoted to the so-called Migration Based Travel Times (MBTT) formulation of the data misfit functional. This approach relies on the decomposition of a velocity model onto two subspaces – smooth propagator and rough depth reflectors. On this base the modified data misfit functional is introduced and compared with standard least squares formulation. Numerical Singular Value Decomposition proves that these two formulations produce functionals which have almost orthogonal stable subspaces. As is well known the classical formulation leads to stable subspaces mainly made of fast oscillating functions (reflectors). At the same time we prove that MBTT modification ensures appearance of the propagator in these stable subspaces.

Numerical experiments prove the feasibility of full inversion for reflected waves in this modified reformulation for the well known Gullfaks velocity model.

Introduction

The velocity model in the depth domain is responsible for correct travel-times of wave propagation and therefore is a key element of the up-to-date seismic data processing. As early as the middle of 80th of the last century A.Tarantola introduced the Full Waveform Inversion (FWI) based on the matching the observed and the synthetic seismograms. The L_2 norm is widely used for such matching, though other criteria are also considered. To minimize the misfit function and to find the elastic parameters of the subsurface, iterative gradient-based algorithms are usually applied. Such approach to FWI proposed originally by Lailly (1983) and Tarantola (1984) has been developed and studied in a great number of publications (see Virieux and Operto (2009), and the references therein).

However, the straightforward application of FWI reconstructs reliably only the reflectivity component of the subsurface but fails to provide a smooth velocity model (see, e.g., (Gauthier et al., 1986) and (Mora, 1988)). The matter is the shape of the data misfit functional differs a lot with respect to various velocity components – it is nearly quadratic with respect to reflectors, but perturbations of the smooth velocity component (propagator) lead to a very complicated and non-linear behavior (see e.g. Sirgue, 2006). Heuristically it is explained by the so-called "cycle-skip" problem when phase shifts of the observed and synthetic data may result in local minima. To mitigate this problem Bunks et al. (1995) proposed a multiscale inversion strategy in which the frequency of the input data is increased progressively. It was implemented by low-pass band filtering of data in the time domain. In frequency-domain FWI (Pratt et al., 1998), one may proceed sequentially from low to high frequencies, which is a very natural and cost-efficient way of applying the approach. The inversion result obtained with lower frequency becomes an initial guess for inversion for the higher frequency constituent of the data, and so on. However, such sequential inversion approach also fails due to lack of low frequencies in the data (Sirgue, 2006). The missing of low-frequency component in the spectrum of the observed waveforms was found out to be critical for successful inversion. This was one of the factors impeding the application of FWI to real data. Recent advances in seismic acquisition and bandwidth broadening, as well as increase in computational power and complication of exploration and production gave a new impetus to the FWI approach. Although the key focus today is on tuning of the forward and inversion processes and on efficiency enhancement of the algorithms, developing approaches which can avoid necessity of extremely low frequencies in the data and provide reasonable grounds for Full Waveform Inversion are of great importance.

In what follows we are concentrated on comparative numerical analysis of the Singular Value Decomposition of the data misfit functional for Full Waveform Inversion in the standard and Migration Based Travel Time formulation which was introduced in (Clement, Chavent and Gomez, 2001).

Method and Theory

Seismic inverse problem can be treated as a nonlinear operator equation:

$$F(m) = d, \qquad (1)$$

where $F: M \rightarrow D$ is a nonlinear forward map, which transforms model space M into data space D. In order to simplify the mathematics below the Helmholtz equation is dealt with:

$$\Delta u + \frac{\omega^2}{c(x)^2} u = f(\omega)\delta(x - x_S) \qquad (2)$$

In (1) the data d are the solution of this equation taken at receivers' position.

Standard least-squares formulation.

The standard approach to Full Waveform Inversion (Tarantola, 1984; Virieux and Operto, 2009) is to find the minimum point of the non-linear data misfit functional (nonlinear least squares formulation):

$$m_* = \underset{m}{\operatorname{argmin}} \; \|F(m) - d\|_D^2 \qquad (3)$$

The common way to search for minimum m_* is implementation of some local minimization technique which usually relies on gradient representation on the base of the adjoint to the linearized forward map (formal Frechet derivative of the full forward map (1)) (Tarantola, 1984).

Migration Based Travel Time (MBTT) formulation.

The essence of this formulation is to decompose the velocity model into two constituents: smooth propagator p and oscillating reflector r (Chavent et al., 2001). In turn, reflector is treated as the result of *true amplitude migration* applied to the part of the data called *time reflectivity* (preimage of the spatial reflector):

$$m = p + r = p + \mathrm{M}(p) < s > \tag{4}$$

The key moment of this decomposition is propagator-reflector interrelation $r = M(p) < s >$ with operator $M(p)$ being some kind of true-amplitude prestack migration/linearized inversion. In particular reweighted version of adjoint operator based migration:

$$\mathrm{M}(p) < s >= W \circ \mathrm{Re} \left\{ DF^{*}(p) < s > \right\} \tag{5}$$

Where DF is Frechet derivative of the full nonlinear map F, * means adjoint operator and W is some linear operator providing true amplitudes imaging/migration.
This kind of the model space decomposition leads to the following modified data misfit functional:

$$\varphi(p,r) = \left\| F(m = p + M(p) < s >) - d \right\|_{D}^{2} \tag{6}$$

Minimization with respect to propagator p and reflector r is performed independently and by turn. We start with admitting $s=d$ and do search for some intermediate value of propagator p. After stabilization of this process the search is switched to time reflectivity s and so on.

Doing the standard computations we come to the following formal gradients with respect to propagator p and time reflectivity s (let us pay attention that computation of space reflectivity r is straightforward by applying (4) and (5)):

$$\nabla_{s} = \mathrm{M}^{*}(p) \left\langle \left(\frac{\delta F}{\delta m}(m) \right)^{*} < F(m) \quad d > \right\rangle \tag{7}$$
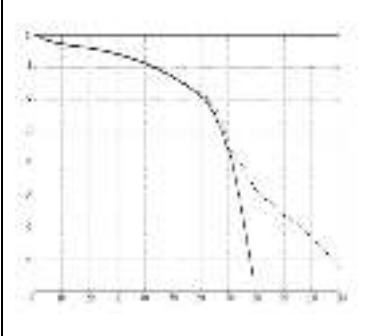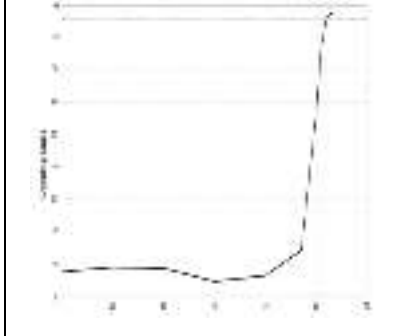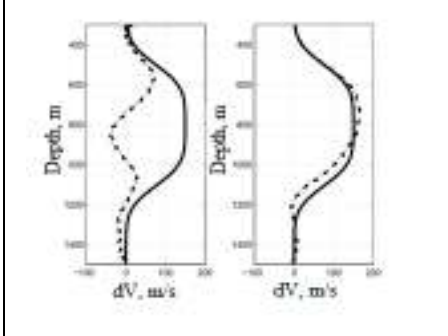
$$\nabla_{p} = \mathrm{Re} \left\{ \left(\frac{\delta F}{\delta m}(m) \right)^{*} < F(m) - d > + \frac{\delta^{2} F}{\delta m^{2}}(p) \left\langle \cdot, W^{*} \circ \left(\frac{\delta F}{\delta m}(m) \right)^{*} < F(m) - d > \right\rangle < s > \right\}. \tag{8}$$

Comparative analysis of the Singular Value Decompositions for standard and MBTT formulations

The main features of the iterative minimization process for both standard and MBTT formulations are governed by the structure of the linearized forward map (formal Frechet derivative). This structure is completely described by the Singular Value Decomposition of the corresponding operators (Cheverda, Kostin, 1995; Silvestrov et al., 2013). Therefore the first series of numerical experiments was devoted to the comparison of SVD for both this formulations. Let us start with Fig.1, representing behavior of singular values. As one can see, they are the same up to number 60 that is up to cond number ≈100.
Next, let us analyze how far apart are linear spans of the right singular vectors of these two Frechet derivatives. To do this we compute opening angles between these linear spans with increasing dimensions. The result is presented in Fig.2 and proves that subspaces are almost the same up to dimension about 50 – 55 but becomes almost orthogonal when spanning more than 60 right singular vectors.
To estimate how linear spans corresponding to reasonable cond numbers (cond≈1000) are situated in the model space with respect to the propagator the simplest propagator is projected to two linear spanned of 70 right singular vectors. In Fig. 3 we present results obtained for standard (left) and MBTT (right) formulations. One can clear see that for the latter propagator is almost perfectly saved, while for the first formulation it is destroyed.

Figure 1 *Singular values for standard (solid line) and MBTT (dashed line) formulations.*

Figure 2 *Opening angles between linear spans of right singular vectors for standard and MBTT formulations.*

Figure 3 *Projection of the propagator to the linear spans of first 70 right singular vectors.*

Numerical Examples for the Realistic Synthetic Models

The realistic example invoked in the study is based on a synthetic velocity model for the Gullfaks South fields presented in Fig. 4a (Thompson, 2003). Input data are synthesized for the set of eighteen uniform frequencies in the range $5 \div 20$ Hz. Our choice of the lowest temporal frequency equal to 5 Hz is due to some publications and discussions real field data range of the stable registration of the signal recording. The acquisition system has 20 volumetric sources and 200 receivers located at depth 10m with a lateral spacing of 200m and 20m respectively. As initial guess, smooth vertically heterogeneous model (see Fig. 4b) is used.

The result obtained by the simultaneous conventional least squares FWI for all frequencies can be seen in Fig.4c and Fig.5a. As one can clear recognize standard non-linear FWI fails to reconstruct smooth velocity model (propagator) for chosen frequency range. Recovered model contains mainly the reflectivity component of the solution, but location of target horizons is reconstructed with a sizeable error (see Fig. 5).

The results of Full Waveform Inversion in MBTT formulation are presented in Fig. 4d and Fig.5b. As an initial guess for the *time reflectivity* variable *s* are used the observed data itself, initial *propagator p* model is the same as the previous one used for conventional FWI (see Fig. 3b). The search for propagator is done in the space of 2D B-Splines functions of order 3. This guaranteed that the search is implemented in the **smooth propagator space**. The minimization is performed using the projected conjugate gradient method, where orthogonal projector onto *smooth space* (B-splines) is used as a projection onto the feasible set.

The propagator reconstruction is demonstrated in Fig. 6. One may see that modified data misfit functional is sensitive with respect to the macro velocity model. Moreover, when the *propagator* unknown *p* is updated, the *depth reflectivity r* is updated as well, because of their interrelation through the migration operator: $r = M(p) < s >$. This is clear seen in Fig.2b: the minimization process updates simultaneously both smooth model and depth reflector. As a result, when propagator is close to the true macro velocity model, reflectors are placed in the correct positions.

The final velocity model, recovered by the Full Waveform Inversion MBTT formulation is presented in Fig. 4d and Fig.5b. As one can see, there is excellent general reconstruction – up to "eyeball norm", there is no difference in real and reconstructed 2D model. In order to see the difference we present 1D real and recovered cross-section. There are some small deviations, which, like smoothing the jump at the depth 1000 m and not absolute coincidence of high oscillations below 2000 m.

Conclusions

We present the results of reflection FWI in MBTT formulation in application to a 2D synthetic dataset. The numerical experiments demonstrate sensitivity of the modified least-squares data misfit functional to a smooth constituent of the velocity model, as opposed to a standard least-squares FWI formulation.
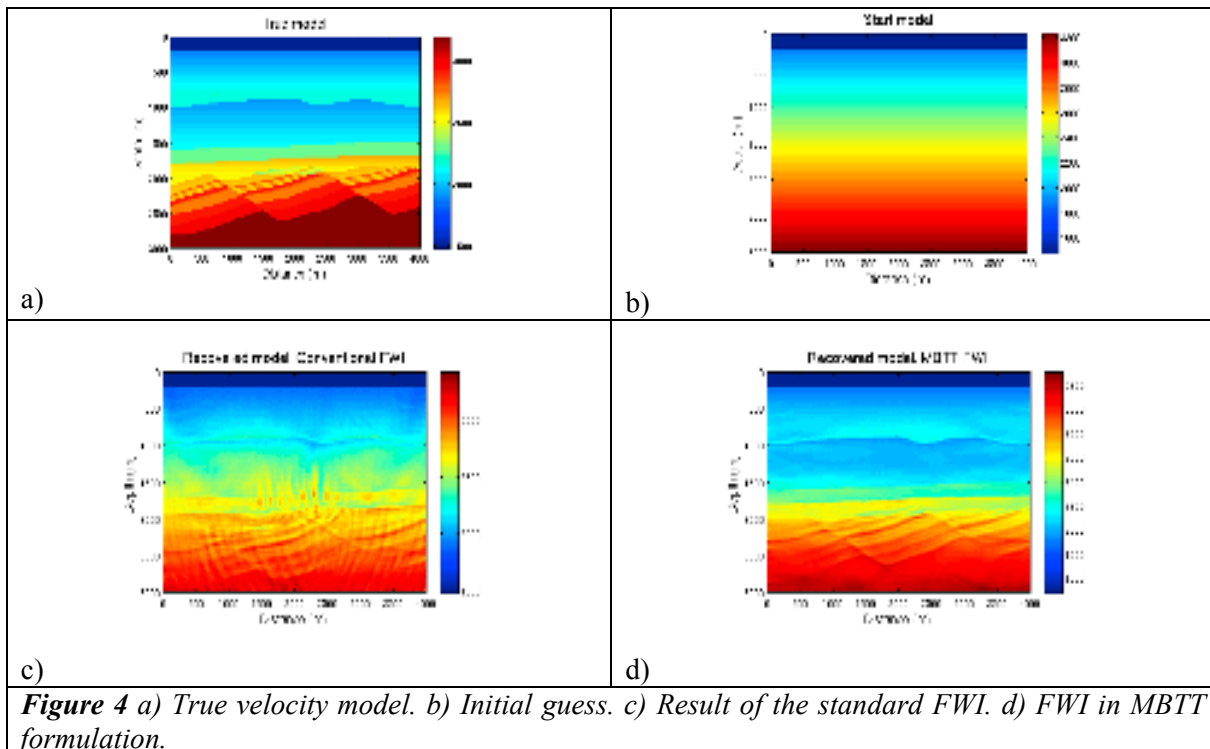
Figure 4 *a) True velocity model. b) Initial guess. c) Result of the standard FWI. d) FWI in MBTT formulation.*

Acknowledgements

References

1. Bunks, C., Saleck, F.M., Zaleski, S. and Chavent, G. [1995] Multiscale seismic inversion. *Geophysics*, **60**(05), 1457-1473.

2. Cheverda, V. and Kostin, V. [1995] R-pseudoinverses for compact operators in Hilbert spaces: existence and stability. *Journal of Inverse and Ill-Posed Problems*, **3**(2), 131-148.

3. Clement, F., Chavent, G. and Gomez, S. [2001] Migration-based traveltime waveform inversion of 2-D simple structures: A synthetic example. *Geophysics*, **66**, 845-860.

4. Gauthier, O., Virieux, J., Tarantola, A. [1986] Two-dimensional non-linear inversion of seismic waveforms – numerical results. *Geophysics*, **51**(7), 1387-1403.

5. Lailly, P. [1983] The seismic inverse problem as a sequence of before stack migrations. Conference on Inverse Scattering: Theory and Application. *SIAM*. 206-220.

6. Mora, P. [1988] Elastic wavefield inversion of reflection and transmission data. *Geophysics*. **53**(6), 750-759.

7. Pratt, G., Shin, C., Hicks, G.J. [1998] Gauss-Newton and full Newton methods in frequency-space seismic waveform inversion. *Geophysical Journal International*, **133**(2), 341-362.

8. Silvestrov, I., Neklyudov, D., Kostov, C., Tcheverda, V. [2013] Full Waveform Inversion for Macro Velocity Model Reconstruction in Look-Ahead Offset VSP. *Numerical SVD-based Analysis*, **61**(6), 1099-1113.

9. Sirgue, L. [2006] The importance of low frequencies and large offset in waveform inversion. *68th EAGE Technical conference and Exhibition*, A037.

10. Tarantola, A. [1984] Inversion of seismic reflection data in the acoustic approximation. *Geophysics*, **49**(8), 1259-1266.

11. Thompson, M., Arnsten, B., Amundsen, L. [2003] Acquisition geometry versus 4C image quality: A study from Gullfaks South. *SEG Technical Program Expanded Abstracts*, **22**(1), 793-796.

12. Virieux, J., Operto, S. [2009] An overview of full-waveform inversion in exploration geophysics. *Geophysics*, **74**(6), WCC1-WCC26.